photoelectrode is a most desirable feature if a high efficiency is to be obtained. A strongly absorbing dye layer on the photoelectrode is one way to meet this requirement. Secondly, Albery and Archer suggest that, if only one electrode is "poisoned" with respect to one redox couple (either the dye couple or the inorganic couple) by adsorbed material, a higher efficiency can be produced. The dye layer on the photoelectrode may well act in this way, and there is evidence4 to this effect in the iron-thionine cell. A third possibility is that the dye layer may constitute a semiconductor electrode with markedly different electrode processes from those which occur at metal electrodes. The latter possibility has particular credibility in the case of thick layers, but further work would be necessary to evaluate the relative merits of the above explanations in the present case.

# Conclusions

It was found that dye layers could be successfully deposited from aqueous rhodamine B solutions onto gold electrodes held at oxidizing potentials between 0.85 and 1.05 V relative to a saturated calomel electrode. The dye layers thus formed ranged in color from orange-red to deep purple and ranged in thickness from ca. 1 to 60 nm.

Absorption, fluorescence, and fluorescence excitation spectra indicated that two different substances were commonly present in the dye layers, these being rhodamine B and its deethylated form, rhodamine 110. Some layers were composed mainly of one of these substances while others contained a mixture of the two, and more control of the deposition conditons would appear to be necessary if a predictable composition is to be produced.

Photovoltage action spectra for dye-coated electrodes were found to resemble the absorption spectra of the several electrodic dye mixtures of rhodamine B and rhodamine 110, although a photovoltage peak at 400 nm is not obviously reflected in the absorption spectrum.

The best power conversion efficiency obtained for a gold-rhodamine B photoelectrochemical cell containing a dye-coated electrode was  $(3.37 \pm 0.5) \times 10^{-4}\%$ . This represented a 14-fold increase on the efficiency of a corresponding cell containing an uncoated gold photoelectrode. Electrochemically deposited dye layers may provide a useful means of improving the efficiencies of other photoelectrochemical cells which are already more efficient than the gold-rhodamine B cell.

Acknowledgment. We thank Mr. S. M. Trotman of our Department and Dr. R. J. Marcus, of the Office of Naval Research, United States Embassy, Tokyo, for a number of helpful discussions during the course of this work. The Department of Pharmacology of the University of Western Australia is thanked for making the spectrofluorimeter available.

# Crystal Structure and Structure-Related Properties of ZSM-5

D. H. Olson, \* G. T. Kokotailo, S. L. Lawton,

Mobil Research and Development Corporation, † Princeton, New Jersey 08540, and Paulsboro Laboratory, Paulsboro, New Jersey 08066

and W. M. Meler

Institute of Crystallography, ETH Zurich, Switzerland (Received: January 15, 1981; In Final Form: April 20, 1981)

A single crystal X-ray study of an as-synthesized ZSM-5 (Si/Al = 86) material having apparent orthorhombic symmetry Pnma and cell parameters a = 20.07, b = 19.92, and c = 13.42 Å has been carried out. The framework topology found agrees with earlier more general descriptions. The three-dimensional channel system consists of straight channels running parallel to [010] having 10-rings of ca. 5.4 × 5.6 Å free diameter and sinusoidal channels running parallel to [100] having 10-ring openings of ca. 5.1 × 5.4 Å. Diffusion in the [001] direction is achieved by movement between these two channels. The structural network can be derived from secondary building units consisting of 12 tetrahedra. The influence of pore structure on hydrocarbon sorption, hydrocarbon product selectivity, and catalyst aging is described.

## Introduction

ZSM-51 is a representative member of a new class of high-silica zeolites having considerable significance as catalyst materials. Examples of their uses include the conversion of methanol to gasoline, dewaxing of distillates, and the interconversion of aromatic compounds.2 Also, ZSM-5 has been shown to possess unusual hydrophobicity, leading to potential applications in the separation of hydrocarbons from polar compounds, such as water and al-

The framework structure and structural features of ZSM-5 have been described previously.4 Herein we report

the crystal structure analysis of ZSM-5, describe the principal features of the structure, and discuss important structure-dependent properties.

# Experimental Section

A ZSM-5 preparation containing large crystals was synthesized by using established procedures. SEM mi-

<sup>(1) (</sup>a) Argauer, R. J.; Landolt, G. R. U.S. Patent 3 702 886, 1972. (b) Dwyer, F. G.; Jenkins, E. E. U.S. Patent 3 941 871, 1976. (2) (a) Meisel, S. L.; McCullough, J. P.; Lechthaler, C. H.; Weisz, P. B. Chem. Technol. 1976, 6, 86. (b) Chang, C. D.; Silvestri, A. J. J. Catal. 1977, 47, 249. (c) Chen, N. Y.; Gorring, R. L.; Ireland, H. R.; Stein, T. R. Oil Gas J. 1977, 75, 165. (3) Chen, N. Y. U.S. Patent 3 732 326, 1973. (4) Kokotailo, G. T.; Lawton, S. L.; Olson, D. H.; Meier, W. M. Nature (London) 1978, 272, 437

<sup>(</sup>London) 1978, 272, 437.

<sup>&</sup>lt;sup>†</sup>P.O. Box 1025.

croanalysis of individual 20 × 30 × 40 µm crystals gives a probable anhydrous composition of MrAl, Sigg 90, 192, where M represents a mixture of sodium and tetraalkyl cations. While the latter could not be quantified, the

analysis indicates 0.8 wt % sodium.

Weissenberg and precession X-ray photographs showed orthorhombic symmetry with k + l = 2n for 0kl, and h =2n for hk0 indicating Pnma to be the space group representing the framework symmetry. The true symmetry is frequently lower than the apparent space group, pseudosymmetry being a well-known phenomenon in zeolite materials. Indeed, apparent monoclinic symmetry has been observed for ZSM-5-type materials. 5,6 Unit cell parameters of the air-equilibrated, as-synthesized material were found to be  $a = 20.07 \pm 0.01$ ,  $b = 19.92 \pm 0.01$ , and  $c = 13.42 \pm 0.01$  Å. The calculated anhydrous framework density is  $1.785 \text{ g/cm}^3 \text{ or } 17.9\text{T}/1000 \text{ Å}^3 \text{ (T = Si or Al)}$ .

Intensity data were collected by manual and automatic procedures on Siemens diffractometers equipped with a GE quarter-circle Eulerian cradle. A total of 1026 observed intensities having  $F_0 > 3\sigma_F$  were measured by using Ni-

filtered Cu Ka radiation.

The sorption measurements were made on a computer-controlled Du Pont 951 TGA. The sorption volumes were computed from the weight measurements using the following liquid densities in g/cm<sup>3</sup>: 0.650 (30 °C) and 0.571 (90 °C) for n-hexane; 0.644 (30 °C) and 0.585 (90 °C) for 3-methylpentane; 0.878 (30 °C) and 0.806 (90 °C) for benzene; 0.871 (30 °C) and 0.820 (90 °C) for o-xylene; and 0.850 (30 °C), 0.813 (70 °C), and 0.785 (90 °C) for p-xylene.

#### Solution of the Structure and Refinement

A combination of trial model building and direct methods was used to solve the structure. Various pieces of information were used to guide the former. Among the more important were unit cell size and space group, distribution and orientation of T-T vectors in Patterson maps, and the indication from hydrocarbon sorption experiments that the zeolite contained 10-membered rings of tetrahedra. Among many other trial structures, five models were developed from heulandite units joined together through an edge. Atom coordinates obtained from these models were refined with the distance least-squares program, DLS,8 which adjusts the coordinates to fit prescribed T-O bond distances and angles within the constraints imposed by the space groups and the cell dimensions. However, in most instances the latter could not be upheld for DLS to proceed. This criterion proved to be an effective way of evaluating possible models. Nevertheless, X-ray powder patterns computed from these theoretical coordinates showed for one of these models a noteworthy similarity with that of ZSM-5.

Application of direct methods resulted in another model which yielded a calculated powder pattern also resembling that observed for ZSM-5. This model possessed structural

units found in mordenite and ferrierite.

The final model was produced by introducing new T-O linkages in these models and contained features in common with both of the former models. DLS showed the cell dimensions to agree with those observed, and the resultant coordinates lead to a calculated diffraction pattern which agreed very closely with the experimental ZSM-5 diffrac-

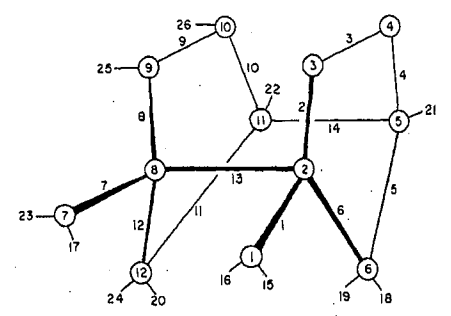


Figure 1. Numbering scheme of the framework atoms.

tion patterns of various ZSM-5 samples.

The DLS coordinates of the ZSM-5 model were used as first cycle coordinates in least-squares refinement. The final R value  $(\sum |F_0 - |F_0|)/\sum F_0$  after 14 cycles was 0.119. The goodness-of-fit parameter,  $\left[\sum w(F_0 - |F_c|)^2/(m-s)\right]^{1/2}$ , equals 1.074, where m is the number of observations and s the number of variables in the least-squares refinement. Only two nonframework peaks, labeled Ox1 and Ox2, were observed in difference Fourier maps. They were refined by using oxygen scattering factors. No definite assignment appeared justified on the basis of interatomic distances and other criteria.

#### Results and Discussion of the Framework Structure

Final atomic coordinates, thermal parameters, and standard deviations are given in Table I. The relatively high standard deviations are a consequence of the small crystal size, which greatly limited the obtainable data set. Occupancy factors obtained for the nonframework atoms were 0.38 (5) for Ox1 and 0.21 (4) for Ox2. The numbering of the framework atoms in the asymmetric unit is shown in Figure 1.

The resultant T-O distances are presented in Table II. (See paragraph at end of text regarding supplementary material.) For a given tetrahedron these bond distances as well as the O-T-O angles are for the most part within  $2\sigma$  and all are within  $3\sigma$  of their respective average value. The overall value of the T-O bond distances is 1.59 (1) Å and agrees remarkably well with mean values recorded for various silica polymorphs. The correlation of T-O distances and T-O-T angles follows the relationship by Gibbs

et al.9 for silica structures.

The T atoms of the ZSM-5 crystal used are practically all Si. Even if the Al atoms present were all concentrated in just one of the T positions, this would only amount to  $\sim$  1/8 of that position which would still be hardly detectable by ordinary X-ray crystal structure refinement. Partially refined atomic coordinates were reported for the silica end member of the ZSM-5 compositional series referred to as "Silicalite". 10 Since many of the T-O distances calculated from those coordinates are clearly outside the acceptable range, 11 a detailed comparison with the results presented here would not seem meaningful although there is general agreement with respect to the basic features of the

<sup>(5)</sup> Wu, E. L.; Lawton, S. L.; Olson, D. H.; Rohrman, Jr., A. C.; Kokotailo, G. T. J. Phys. Chem. 1979, 83, 2777.
(6) Bennett, J. M.; Cohen, J. P.; Kirchner, R. M. A.C.A. Meet. Abstr.

<sup>(7)</sup> Venuto, P. B.; Cattanach, J.; Landolt, R. L., unpublished research,
Mobil Research and Development Corp., Paulsboro, NJ.
(8) Meier, W. M.; Villiger, H. Z. Kristollogr. 1969, 129, 411.

 <sup>(9)</sup> Hill, R. J.; Gibbs, G. V. Acta Crystallogr., Sect. B 1979, 35, 25.
 (10) Flanigan, E. M.; Bennett, J. M.; Grose, R. W.; Cohen, J. P.;
 Patton, R. L.; Kirchner, R. M.; Smith, J. V. Nature (London) 1978, 217,

<sup>512.
(11)</sup> Reported atom coordinates in ref 10 lead to Si-O distances as low as 1.20 Å and as high as 2.65 Å. Strong correlations between positional parameters related by pseudosymmetry elements must have led to the doubtful atom coordinates in the reported structure refinement using space group Pn2<sub>1</sub>a. Symmetrization of these atom coordinates to Pnma results in Si-O distances which differ considerably less from expected values according to a personal communication by J. V. Smith.

TABLE I: Positional and Thermal Parameters for ZSM-5

atom	position	x	У	z	B, A <sup>2</sup>
T1	8d(1)	0.4232(5)	0.0605 (7)	-0.3306 (9)	1.0 (3)
T2	8d(1)	0.3090 (9)	0.0281 (5)	-0.1849 (11)	1.9 (3)
T3	8d(1)	0.2788 (5)	0.0602 (8)	0.0312 (10)	2.1 (3)
T4	8d(1)	0.1220(6)	0.0641 (7)	0.0326 (9)	1.4 (3)
<b>T</b> 5	8d(1)	0.0728 (7)	0.0278 (6)	-0.1822(13)	1.9 (3)
$\mathbf{T6}$	8d(1)	0.1884 (8)	0.0573 (7)	-0.3249(9)'	2.0 (3)
$\overline{\mathbf{T7}}$	8d(1)	0.4232 (7)	-0.1695 (7)	-0.3258(13)	2.7 (3)
T8	8d(1)	0.3076 (9)	-0.1286(7)	-0.1848 (11)	2.2 (3)
T9	8d(1)	0.2748 (6)	-0.1722(6)	0.0366 (10)	1.6 (3)
T10	8d(1)	0.1199 (6)	-0.1729 (6)	0.0269 (10)	1.8 (3)
T11	8d(1)	0.0702 (6)	-0.1304(6)	-0.1826 (10)	1.0 (3)
T12	8d(1)	0.1894 (8)	-0.1742 (5)	-0.3172(9)	1.2 (2)
01	8d(1)	0.3728(14)	0.0665 (15)	-0.2397(19)	2.8 (6)
O2	8d(1)	0.3095 (13)	0.0621 (12)	-0.0761(13)	1.7 (5)
O3	8d(1)	0.1993 (18)	0,0605 (16)	0.0263 (18)	5.4 (6)
O4	8d(1)	0.1000 (15)	0.0571 (26)	-0.0817 (23)	4.9 (8)
· O5	8d(1)	0.1183 (10)	0.0592 (15)	-0,2697 (13)	0.8 (4)
06	8d(1)	0.2407 (14)	0.0440(16)	-0.2418(21)	3.6 (7)
07	8d(1)	0.3750 (15)	-0.1509 (16)	-0.2361(21)	3.0 (7)
08	8d(1)	0.3079 (18)	-0.1514 (11)	-0.0681 (17)	3.0 (6)
09					3.7 (5)
	8d(1)	0.1981 (17)	-0.1541 (10)	0.0324 (17)	
010	8d(1)	0.0909 (16)	-0.1652 (18)	-0.0751(25)	4.4 (9)
011	8d(1)	0.1230 (18)	-0.1427(22)	-0.2632(26)	6.1 (9)
012	8d(1)	0.2529 (14)	-0.1660 (14)	-0.2393 (21)	2.9 (7)
O13	8d(1)	0.3112 (17)	-0.0519 (21)	-0.1823 (20)	5.6 (7)
· 014	8d(1)	0.0790 (12)	-0.0526(22)	-0.1743 (20)	4.4 (6)
015	8d(1)	0.4091 (13)	0.1258 (15)	-0.3870(21)	2.9 (6)
O16	8d(1)	0.4160 (15)	0.0011 (18)	-0.4177(24)	4.0 (8)
017	8d(1)	0.3976 (15)	-0.1300 (16)	-0.4191 (22)	3.1 (7)
O18	· 8d(1)	0.1847 (11)	0.1295(12)	-0.3824(16)	1.3 (5)
019	8d(1)	0.2037 (16)	0.0030 (15)	-0.4020(22)	3.2 (7)
020	8d(1)	0.1910(20)	-0.1259(17)	-0.4147(22)	4.9 (8)
021	8d(1)	-0.0016(12)	0.0425 (13)	-0.2056 (19)	1.9 (6)
022	8d(1)	-0.0016 (14)	-0.1565 (13)	-0.2078(20)	1.9 (6)
O23	4c(m)	0.4277 (19)	-0.25	-0.3503 (28)	2.4 (9)
O24	4c(m)	0.2045 (17)	-0.25	-0.3476(23)	1.4 (7)
O25	4c(m)	0.2861(14)	-0.25	0.0590 (23)	0.5 (7)
O26	4c(m)	0.1089 (23)	-0.25	0.0580 (34)	2.7 (11)
Ox1	4c(m)	0.1746 (33)	0.75	0.3515 (50)	0.7
Ox2	4c(m)	0.3770 (68)	0.75	0.3790 (94)	0.7
	O Distances (A ) f				
T1-01	<del></del>	9 (3) T5-O4	1.57 (4)	T9-08	1.61 (3)
T1-01		3 (3) T5-O5	1.61 (3)	T9-O9	1.58 (4)
T1-01		7 (3) T5-O14	1.61 (5)	T9-O18	1.60(2)
T1-02		2 (3) T5-O21	1.55 (3)	T9-O25	1.59 (2)
11 02	av 1.6		av 1.58 (2)	10 020	av 1.60 (1)
T2-O1				m10 00	
			1.59 (2)	T10-O9	1.62 (4)
T2-O2	1.0	1 (2) T6-06	1.56 (3)	T10-O10	1.50 (4)
T2-O		0 (3) T6-O18	1.63 (3)	T10-O15	1.60 (3)
T2-O1	1.6	30 (4) T6-O19	1.53(3)	T10-O26	1.61 (2)
	av 1.6	32 (2)	av 1.58 (1)		av 1.58 (2)
T3-O2	1.5	57 (2) T7-O7	1.59(3)	T11-O10	1.65 (4)
T3-O3	3 1.6	50 (4) T7-O17	1.57 (4)	T11-O11	1.53 (4)
T3-O1		8 (3) 177-022	1.60 (3)	T11-O14	1.56 (5)
T3-O2		1 (4) T7-O23	1.64(2)	T11-O22	1.57 (3)
9.	av 1.8		av $1.60(2)$	<b></b>	av 1.58 (2)
T4-03		66 (4) T8-O7	1.58 (4)	T12-O11	1.64 (4)
T4-04	1 1.0	30 (3) T8-O8	1.68 (3)	T12-O11	1.66 (3)
T4-0		35 (4) T8-O12	1.52 (3)	T12-O20	1.62 (3)
T4-01	1.0	(2 (3) T8-O13	1,53 (4)	T12-O24	1.59 (1)
1.0.		- 120			

Average T-O = 1.59 (1)

av 1.56 (2)

structure in line with earlier reports<sup>2a,4</sup> presenting less detail.

The secondary building unit (SBU) of the framework is most adequately considered to comprise 12 T atoms and is shown in Figure 2a. 12 Such building units must be topologically nonchiral or else left- and right-handed

should also be evident from Figure 2a that this SBU can be readily described as a pair of five 1-units.

These SBUs can be linked to form chains as shown in Figure 2b. Such a chain can simply be generated by ap-

components must be distinguished when assembling the framework. Other units of 12 T atoms were also examined

but had to be ruled out on the basis of this criterion. 13 It

av 1.63 (2)

<sup>(12)</sup> It was also considered convenient to adopt essentially the SBU as the asymmetric unit (Figure 1) of the structure since the space group  ${\it Pnma}$  allows this.

<sup>(13)</sup> Kokotailo, G. T.; Meier, W. M. Chem. Soc., Spec. Publ. 1980, 33, 133.

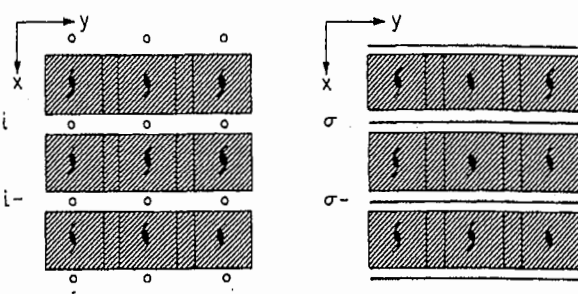


Figure 4. Stacking sequences of layers in ZSM-5 and ZSM-11 (layers shaded).

(b)

Figure 2. Secondary building unit (a) and chain-type building block (b).

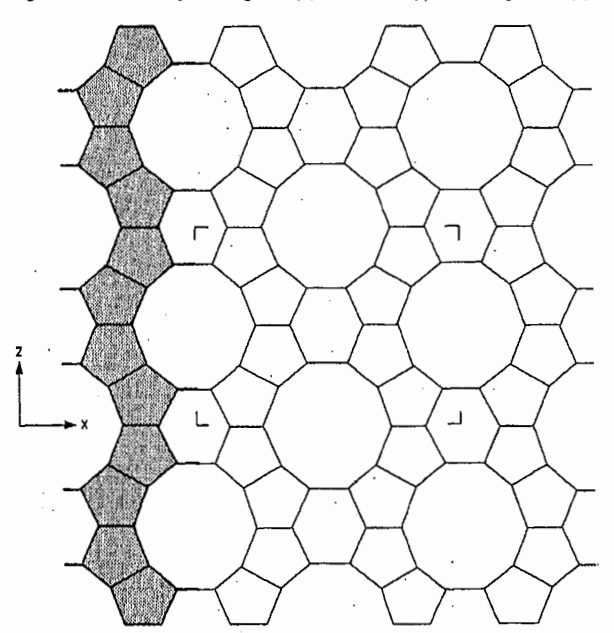


Figure 3. Skeletal diagram of ZSM-5 layer with chains of Figure 2b outlined.

plying the operations of a 2-fold screw axis to a SBU. Such chains can then be interconnected to form a layer as outlined schematically in Figure 3. Neighboring chains in these layers are related by mirrors. The ZSM-5 layer shown diagrammatically in Figure 3 has been recognized to be the basis of a very useful scheme for characterizing a series of closely related structures. <sup>13</sup> Pairs of such layers can be interconnected in two ways. When connected, neighboring layers are either related by the operations of a mirror  $(\sigma)$  or by an inversion (i). The latter applies to ZSM-5 as illustrated in Figure 4, whereas mirrors occur in the similar structure of ZSM-11. <sup>14</sup> Any number of possible structures can be readily postulated when com-

(14) Kokotailo, G. T.; Chu, P.; Lawton, S. L.; Meier, W. M. Nature (London) 1978, 275, 119. binations of the two operations,  $\sigma$  and i, are considered. The operations  $\sigma$  and i involve only neighboring layers and therefore need not be crystallographic symmetry operations. ZSM-5 and ZSM-11 are the structural end members of an essentially continuous series of "intermediate" structures which has been called the Pentasil series. Errors in an ideal  $(\sigma, i)$  sequence are to be expected in such structures and could of course seriously hamper further extensive structure refinements of these phases.

A skeletal projection of ferrierite along [001] looks the same as Figure 3, representing a ZSM-5 layer in projection (or a projection of the ZSM-5 framework structure along [010]). The same diagram is also obtained for the tetragonal framework of ZSM-11 in projection along (100).

ZSM-5 has an effective three-dimensional channel defined by 10-membered ring openings (Figure 5). Straight channels parallel to [010] have openings defined by 10-rings of size  $5.4 \times 5.6$  Å based on oxygen radii of 1.35 Å. Intersecting this channel at right angles is a sinusoidal channel along [100] with openings of  $5.1 \times 5.5$  Å. Diffusion in the [001] direction can readily take place between the overlapping channels parallel to [100] and [010].

## Structure-Related Properties

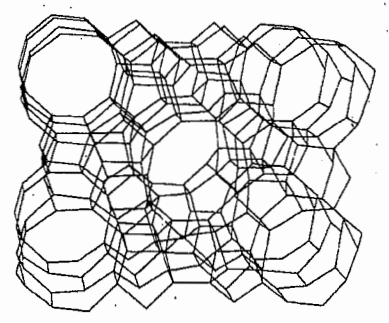
Sorptive Properties. With a channel size intermediate between small pore (8-ring) and large pore (12-ring) zeolites (see Figure 6), ZSM-5 possesses distinct sorption and diffusion properties. Hydrocarbon sorption by 8-ring zeolites is essentially limited to normal paraffins while 12-ring zeolites can sorb molecules as large as tributylamine (9.1 Å). While ZSM-5 sorbs molecules as large as o- and m-xylene, 1,2,4-trimethylbenzene, and naphthalene, all having minimum diameters of  $\sim$ 6.9 Å (see ref 16), they all sorb slowly, indicating steric restrictions. Pentamethylbenzene and 1,3,5-trimethylbenzene ( $\sim$ 7.8 Å) are essentially excluded. In addition to this molecular sieving, the ZSM-5 channel structure imposes intracrystalline steric effects which are revealed in its hydrocarbon sorption isotherms.

Zeolites typically exhibit type I isotherms<sup>17</sup> exemplified by the *n*-hexane and *p*-xylene isotherms in Figure 7a, where hydrocarbon capacity in the plateau region reflects zeolitic pore volume. Hydrocarbon sorption volumes below true pore capacity normally reflect exclusion from certain regions or cages in the structure. However, for benzene, other factors must be involved since *p*-xylene, which has

<sup>(15)</sup> Breck, D. W. "Zeolite Molecular Sieves"; Wiley: New York, 1974; pp 636-7.

<sup>(16)</sup> Strictly speaking, kinetic diameters should be used for both the molecules being sorbed and for zeolitic oxygens used in computing channel sizes. However, lacking these data for all of the species, we have used minimum diameters measured from Courtauld molecular models for hydrocarbon molecule sizes and the conventional value of 1.35 Å for oxygen radius for calculation of channel size.

oxygen radius for calculation of channel size.
(17) Brunauer, S. "The Adsorption of Gases and Vapors"; Oxford University Press: London, 1944; p 150.



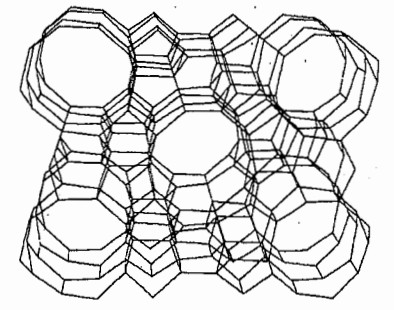


Figure 5. Stereo pair drawing of ZSM-5 framework viewed along [010] (a axis horizontal).

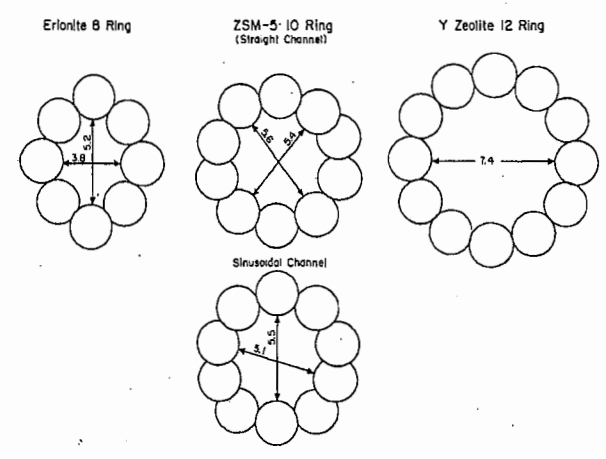


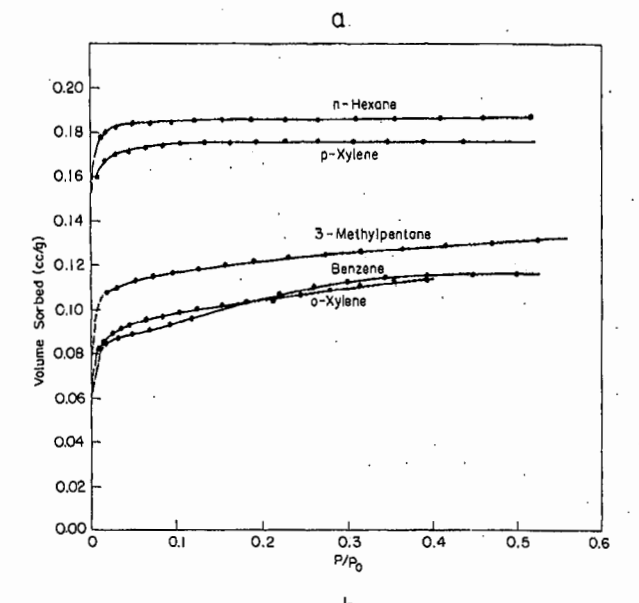
Figure 6. Comparison of the limiting ports of erionite, ZSM-5, and faulasite.

the same minimum cross-sectional area, appears to fill the pores. This difference between benzene and p-xylene is apparently due to the additional interaction forces of the methyl hydrogen atoms as well as entropy contributions resulting from more favorable packing of p-xylene.

The indication of special packing arrangements for p-xylene is supported by the phase transition observed in the 70 °C isotherm (Figure 8). At constant system composition ( $P/P^0 \approx 0.03$ ) the solid phase changes from 4 to  $\sim 6.5$  molecules of p-xylene per unit cell of ZSM-5. The number 4 is significant crystallographically and suggests an ordered packing of the p-xylene molecules. The latter solid phase probably corresponds to pore filling rather than a stoichiometric or ordered p-xylene–ZSM-5 sorption complex.

The high affinity for n-paraffins is demonstrated by the 90 °C isotherms (Figure 7b) where pore filling is achieved at  $\sim P/P^0=0.05$  and the volume sorbed is nearly twice that of p-xylene, benzene, and 3-methylpentane. The latter is also apparently affected by unfavorable packing in the channels. The high normal paraffin affinity is thought to result from the channel geometry affording very favorable paraffin-channel wall interaction (—C-H O<) in which a high percentage of the paraffinic hydrogen atoms are involved. The constancy of the isosteric heat of adsorption ( $\sim$ 20 kcal/mol for n-hexane) contrasts with the more normal decline in isosteric heat with loading and indicates that (paraffin) molecule-zeolite interactions predominate over molecule-molecule interactions even at high loadings.

Influence of Channel Dimensions on Diffusivity. The channel dimension of ZSM-5 (5.4 × 5.6 Å for the straight channel) is similar to the kinetic diameter of benzene 5.8 Å. Thus while benzene has high mobility in ZSM-5, diffusion of meta- and ortho-disubstituted and polysubstituted aromatics is substantially slower (see Table III).



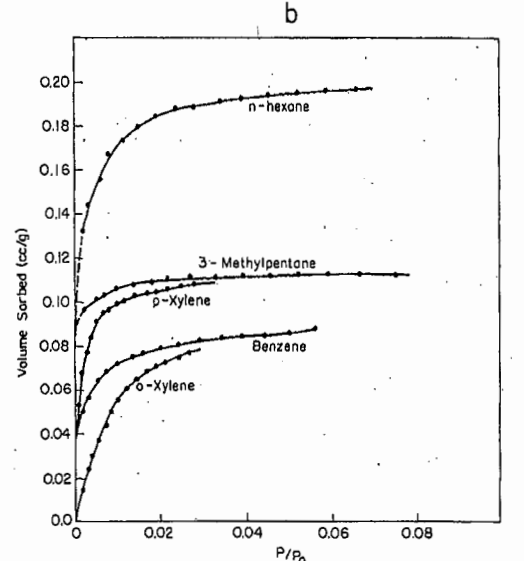


Figure 7. Sorption isotherms for various hydrocarbons on HZSM-5 ( $SiO_2/Al_2O_3 = 290$ ): (a) at 30 °C; (b) at 90 °C.

TABLE III: Diffusivity of Aromatics in ZSM-5a (315°C)

/s ·
t)
•
st)

a Reference 18. b Reference 15.

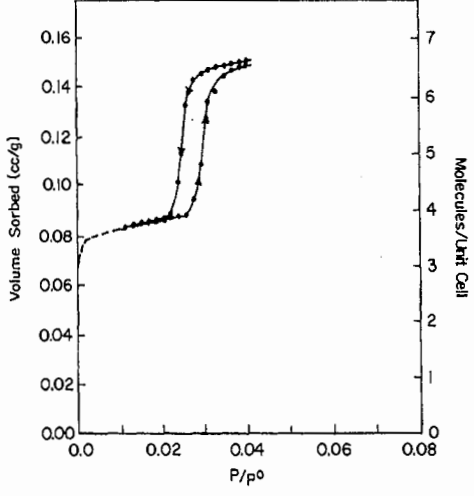


Figure 8. Sorption of p-xylene on HZSM-5 (SIO $_2$ /Al $_2$ O $_3$  = 226) at 70 °C.

For example, the diffusion coefficient for p-xylene, D(pxylene), is  $\sim 3$  orders of magnitude greater than D(o-xylene). As shown below, the similarity of the ZSM-5 channel size and the size of the benzene molecule has a very significant influence on the performance of ZSM-5 catalysts in several potentially important processes.

Influence of Structure on Catalytic Properties. Numerous reactions catalyzed by ZSM-5 reflect the influence of its structure, e.g., having product selectivities and/or aging rates distinctly different from those of larger-pore zeolites such as mordenite- and faujasite-type zeolites. In some of these reactions, steric factors are primarily involved whereas in others diffusion effects play a significant

The steric effects of the ZSM-5 structure are well illustrated by the product distribution in the methanol-to-gasoline process. <sup>2b,18</sup> In this process the reaction proceeds from methanol to olefins to aromatics (primarily polymethylbenzenes). When catalyzed by ZSM-5, less than 1% of the product is heavier than C<sub>10</sub> (tetramethylbenzene) whereas more than 70% of the product is heavier than  $C_{10}$  with a large-pore, mordenite catalyst.<sup>20</sup> The  $C_{10}$  cutoff for ZSM-5 results from steric restrictions which limit formation of heavier (larger) products. Lower diffusivity of the heavier products may also be a factor.

Steric factors are also apparent in paraffin cracking where branched paraffins, e.g., 3-methylpentane, crack slower than their normal paraffin isomers.<sup>21</sup> Over largepore zeolites, mordenite and Y zeolite, the trend is reversed. From a study of C<sub>6</sub> paraffin cracking over ZSM-5, Haag and Lago<sup>22</sup> have shown that steric factors and not diffusional effects are responsible for this cracking selectivity. This selectivity for cracking normal paraffins over branched paraffins has led to the development of a dewaxing process based on ZSM-5 catalysts.2c

Recently, there have been numerous reports<sup>23-27</sup> of high

para selectivity in catalytic reactions producing dialkyl aromatics over pure and modified ZSM-5 catalysts. For example, 88% p-xylene (as percent of xylenes) was obtained from the disproportionation of toluene over a modified ZSM-5 catalyst.27 This result was achieved at conditions where near-equilibrium distribution of xylenes ( $\sim$ 24% para, 54% meta, 22% ortho) would be expected from larger-pore zeolites.

It has been shown that the higher para selectivity is directly related to the low diffusivity of o-xylene relative to p-xylene (discussed above) and that para selectivity may be increased by increasing crystal size or by chemical modification which results in reduced diffusivity. 28,29 Steric factors affecting the primary intracrystalline isomer

distribution may also be important.

Catalyst Aging Properties. ZSM-5-based catalysts have low coke formation and aging rates relative to larger-pore zeolite catalysts. 30,31 While ZSM-5's low aluminum content may contribute to these desirable properties, the size and the architecture of its channel system are believed to be the most important factors.

From a study of faujasite-type catalysts, Venuto et al. 32,33 came to recognize the importance of "reverse molecularsize selectivity" in the aging process of zeolite catalysts. Accordingly, if a zeolite contains cavities or cages with dimensions larger than the ports leading to the crystal exterior, large intracrystalline products, "coke", may form which cannot escape through the ports. Reverse molecular-size selectivity results in aging via pore filling and site blockage. Thus, a zeolite's intrinsic aging rate would be related to how closely its cavity size approaches its port dimensions.

More recently these concepts have been explored extensively and expanded by Rollmann et al. 30,31,34,35 From a systematic study using zeolites having a range of pore sizes, they find that coke formation increases with increasing pore size and that ZSM-5 has significantly lower aging rates than the larger-pore zeolites mordenite and Y. They conclude that the spatial constraints of ZSM-5 are primary factors limiting coke formation. It is possible that numerous structure-dependent properties of ZSM-5 contribute to its low coke-forming and aging rate, limited possibility for "reverse molecular-size selectivity", steric constraints, and multidimensional pore system.

Acknowledgment. W.M.M. acknowledges the support by the Swiss National Science Foundation. We also thank F. G. Dwyer for his role in providing the sample used in the single crystal study and also acknowledge helpful discussions with colleagues G. T. Kerr and W. O. Haag and the experimental assistance of N. H. Goeke.

Supplementary Material Available: An expanded version of Table II, listing interatomic distances and bond angles; Table IV, listing observed and calculated structure factors; and Figure 9, a scatter diagram of T-O bond lengths vs. cosecant of T-O-T angle (7 pages). Ordering information is given on any current masthead page.

3 894 107, 1975.
(20) Chang, C. D., Mobil Research and Development Corp., Princeton,

<sup>(18)</sup> Gorring, R. L., Mobil Research and Development Corp., Princeton, NJ 08540, unpublished research.
(19) Kaeding, W. W.; Jurewicz, A. J.; Butter, S. A. U.S. Patent

<sup>(20)</sup> Chang, C. D., Mobil Research and Development Corp., Frinceton, NJ 08540, personal communication.
(21) Frillette, V. J.; Haag, W. O.; Lago, R. M. J. Catal. 1981, 67, 218.
(22) Haag, W. O.; Lago, R. M., Mobil Research and Development Corp., Princeton, NJ 08540, unpublished research.
(23) Butter, S. A.; Young, L. B. U.S. Patent 3 965 209, June 22, 1976.
(24) Butter, S. A.; Kaeding, W. W. U.S. Patent 3 965 208, June 22, 1978.

<sup>(25)</sup> Chen, N. Y. U.S. Patent 4002697, January 11, 1977.

<sup>(26)</sup> Chu, C. U.S. Patent 4011 276, March 8, 1977. (27) Chen, N. Y.; Kaeding, W. W.; Dwyer, F. G. J. Am. Chem. Soc. (28) Haag, W. O.; Olson, D. H. U.S. Patent 4117026, September 26,

 <sup>(29)</sup> Olson, D. H.; Haag, W. O., in preparation.
 (30) Rollmann, L. D.; Walsh, D. E. J. Catal. 1979, 56, 139.
 (31) Walsh, D. E.; Rollmann, L. D. J. Catal. 1979, 56, 195.
 (32) Venuto, P. B.; Hamilton, L. A. Ind. Eng. Chem. Prod. Res. Dev. 67, 5100. (32) Venuto, P. B. Adv. Chem. Ser. 1971, No. 102, 206. (34) Rollmann, L. D. J. Catal. 1977, 47, 113. (35) Walsh, D. E.; Rollmann, L. D. J. Catal. 1977, 49, 369.